Quaternary Science Reviews 115 (2015) 123–131

Contents lists available at ScienceDirect

Quaternary Science Reviews

journal homepage: www.elsevier.com/locate/quascirev

Combining charcoal sediment and molecular markers to infer a Holocene fire history in the Maya Lowlands of Petén, Guatemala

Simon Schüpbach [a, b, c, *], Torben Kirchgeorg [a, d], Daniele Colombaroli [c, e], Giorgia Beffa [c, e], Marta Radaelli [f], Natalie M. Kehrwald [a], Carlo Barbante [a, f, g]

[a] Department of Environmental Sciences, Informatics and Statistics, University Ca'Foscari, Venice 30123, Italy
[b] Climate and Environmental Physics, Physics Institute, University of Bern, Bern 3012, Switzerland
[c] Oeschger Centre for Climate Change Research, University of Bern, Bern 3012, Switzerland
[d] Institute of Sustainable and Environmental Chemistry, Leuphana University of Lüneburg, Lüneburg 21335, Germany
[e] Institute of Plant Sciences, University of Bern, Bern 3013, Switzerland
[f] Institute for the Dynamics of Environmental Processes-CNR, Venice 30123, Italy
[g] Centro Linceo B. Segre, Accademia Nazionale dei Lincei, Rome 00165, Italy

ARTICLE INFO

Article history:
Received 20 November 2014
Received in revised form
9 March 2015
Accepted 10 March 2015
Available online

Keywords:
Holocene
Guatemala
Biomass burning
Climate
Human activities
Sedimentary charcoal
Levoglucosan

ABSTRACT

Vegetation changes in the Maya Lowlands during the Holocene are a result of changing climate conditions, solely anthropogenic activities, or interactions of both factors. As a consequence, it is difficult to assess how tropical ecosystems will cope with projected changes in precipitation and land-use intensification over the next decades. We investigated the role of fire during the Holocene by combining macroscopic charcoal and the molecular fire proxies levoglucosan, mannosan and galactosan. Combining these two different fire proxies allows a more robust understanding of the complex history of fire regimes at different spatial scales during the Holocene. In order to infer changes in past biomass burning, we analysed a lake sediment core from Lake Petén Itzá, Guatemala, and compared our results with millennial-scale vegetation and climate change available in the area. We detected three periods of high fire activity during the Holocene: 9500–6000 cal yr BP, 3700 cal yr BP and 2700 cal yr BP. We attribute the first maximum mostly to climate conditions and the last maximum to human activities. The rapid change between burned vegetation types at the 3700 cal yr BP fire maximum may result from human activity.

1. Introduction

Fire in the earth system plays an important ecological role by influencing biogeochemical and carbon cycles, atmospheric chemistry, aerosols, land-surface properties and human activities on a local to a global scale (Carcaillet et al., 2002; Bowman et al., 2009). Climate conditions such as moisture levels and temperature control fire activity through biomass accumulation and the likelihood of its spread. In turn, biomass burning influences climate at a more global scale by the emission of aerosols and greenhouse gases, like carbon dioxide and methane. Humans used fire to clear landscapes at least since the introduction of agriculture, thus influencing the long-term fire variability. Scientists actively debate if such early anthropogenic activities impacted the climate and, if so, when this influence began (Ruddiman, 2003). The potential of fire to affect the climate system is demonstrated by recent carbon dioxide emissions from fire, which account up to 50% of the total emitted carbon dioxide (Bowman et al., 2009).

Evidence of early human agriculture activity in Mesoamerica as early as 7000 BP is based on *Zea mays* pollen in sediment cores from northwest Mexico (Pohl et al., 2007). However, other studies demonstrate that the initiation of maize cultivation varied between different Mesoamerican regions (Pope et al., 2001). The Maya Lowlands, consisting of the Yucatan Peninsula (Mexico) and parts of Guatemala, are known as the center of the rise and fall of the Maya culture. The history of the Maya began ca 4000 BP, and they became the largest and highly developed culture in Mesoamerica until declining rapidly around 900 BP. The literature refers to this

* Corresponding author. Climate and Environmental Physics, Physics Institute, University of Bern, Sidlerstrasse 5, 3012 Bern, Switzerland. Tel.: +41 31 631 44 65.
E-mail address: schuepbach@climate.unibe.ch (S. Schüpbach).

http://dx.doi.org/10.1016/j.quascirev.2015.03.004

population decline as the "*Classic Maya collapse*" which may be due to several severe droughts (e.g. Haug et al., 2003; Kennett et al., 2012).

Pollen records and lake sediment patterns from the Maya Lowlands show a rapid vegetation change (e.g. forest openings, increase in pioneer tree species) and increase of soil erosion during the Holocene and particularly when the Maya were the prominent culture (e.g. Islebe et al., 1996; Leyden, 2002; Anselmetti et al., 2007). The soil erosion resulted in an inorganic sediment layer, the "*Maya Clay*" observed in several sediment cores in the Maya Lowlands (e.g. Curtis et al., 1998; Anselmetti et al., 2007; Mueller et al., 2009). Researchers still discuss if the major driving forces behind this vegetation change and the rapid soil erosion were changing climate conditions or early Maya deforestation. The role of fire, anthropogenic or natural, on this system during the Holocene, was only partly discussed in these studies.

The aim of this study is to reconstruct Holocene fire activity at Lake Petén Itzá and to compare this biomass burning record with previously published multi-proxy studies in Lake Petén Itzá sediment cores and other regional sampling sites for a better understanding of the interaction between climate, humans and fire. In order to reach this aim, we use a novel multi-proxy approach which combines lake sediment macroscopic charcoal (a proxy for biomass burning at local-scale, see (Whitlock and Larsen, 2001)) and concentrations of the monosaccharide anhydrates (MAs) levoglucosan (1,6-anhydro-β-D-glucopyranose), mannosan (1,6-anhydro-β-D-mannopyranose) and galactosan (1,6-anhydro-β-D-galactopyranose) as specific molecular markers for biomass burning in lake sediments (Elias et al., 2001; Conedera et al., 2009; Kuo et al., 2011b; Kirchgeorg et al., 2014). Comparing the two biomass burning proxies may help increase our understanding about advantages and limitations of molecular markers as proxies for past fire reconstruction.

2. Study area

Lake Petén Itzá (17°00′N, 89°50′W, 110 m above sea level) is located in the Department of Petén in the northern part of Guatemala (Fig. 1). It is the deepest lake in the Maya Lowlands of Central America with a maximal depth of approximately 165 m. Previous studies demonstrated that the lake did not desiccate during long dry periods and had a continuous sedimentation (Mueller et al., 2009). Lake Petén Itzá receives water from surface runoff, rainfall, subsurface groundwater, and a small input stream, without any significant outflows (Correa-Metrio et al., 2012). Due to the fact that Lake Petén Itzá receives most of its water by rainfall, the water level strongly depends on rainfall and evaporation. The annual mean temperatures in this region are on average 25 °C with a high variability of precipitation between 900 and 2500 mm yr^{-1}, which occurs mainly between June and October, followed by a dry winter. The climate is quite sensitive to the migration of the Intertropical Convergence Zone (ITCZ), which controls the regional rainfall (Deevey et al., 1980; Hillesheim et al., 2005; Hodell et al., 2008).

Prior to the Maya the vegetation at Lake Petén Itzá was characterized by closed-forest taxa including *Moraceae* and *Urticaceae*. During the occupation of the Maya, the pollen records show a shift to more open vegetation, including *Amaranthaceae*, *Ambrosia*, *Compositae*, *Cyperaceae*, as well as *Poaceae* and other disturbance-adapted taxa, which are assumed to be a result of the deforestation (Curtis et al., 1998; Leyden, 2002; Rosenmeier et al., 2002). These changes were observed at several other sites in the Maya Lowlands (Leyden, 2002). The forest recovered to pre-Maya taxa after the *Classic Maya Collapse*.

The Maya settlements and the beginning of the agricultural activity in Petén was dated around 3000 BP, corroborated by the first findings of *Zea mays* pollen and the beginning of the stratigraphic section of *Maya Clay* in the cores from lakes in Petén (e.g. Wahl et al., 2006; Anselmetti et al., 2007; Mueller et al., 2009). The *Classic Maya Collapse* diminished the Maya population in Petén but historical documents and archaeological studies demonstrate that Lake Petén Itzá was still surrounded by several Maya settlements after the *Classic Maya Collapse* and migration towards the lake may have occurred until the arrival of Spanish conquerors (Rice et al. 1998).

3. Materials and methods

3.1. Samples

The 110 lake sediment samples originate from the core PI 5 VI 02 11B collected in Lake Petén Itzá in June 2002 (Hillesheim et al., 2005). The 11B core is one out of six (11A–11F) piston cores along seismic line 11, recovered using a Kullenberg type piston corer triggered by a mud–water interface corer (Hillesheim et al., 2005; Anselmetti et al., 2006). The 550 cm long core 11B was chosen because it covers the entire Holocene, it is well dated, and various proxy data are available from this or parallel cores from Lake Petén Itzá and from surrounding lakes (e.g. Rosenmeier et al., 2002; Hillesheim et al., 2005; Anselmetti et al., 2006; Mueller et al., 2009; Correa-Metrio et al., 2012). The samples of approximately 5 g wet weight were subsampled from the original core at the University of Florida, USA, and shipped to the University of Venice, Italy in 2012. The subsamples were taken from a depth of 18 to 514 cm. One sample covers a depth of 2 cm. Distance between two samples is 5.5 cm (i.e. 7.5 cm sampling resolution) from 18 to 300 cm depth, and 1 cm (3 cm sampling resolution) from 300 to 514 cm depth. In Venice, samples were divided into two parts: 1 cm^3 of wet sample was used for the macroscopic charcoal analyses, while the remaining sample was freeze-dried and homogenized for molecular biomass burning marker and total organic content (TOC) analyses. As sampling was not contiguous our fire history reflects low frequency changes in biomass burning over the millennial time scale.

3.2. Analytical methods

The monosaccharide anhydrates levoglucosan (1,6-anhydro-β-D-glucopyranose), mannosan (1,6-anhydro-β-D-mannopyranose) and galactosan (1,6-anhydro-β-D-galactopyranose) were analysed using an aliquot of 200 mg of freeze-dried and homogenized sediment. The compounds were extracted by pressurized solvent extraction (PSEone, Applied Separations, Hamilton, USA) with methanol (Ultrapure, Romil LTD, Cambridge, UK), filtered (0.2 μm, PTFE), evaporated to dryness (Turbovap, Biotage, Uppsala, Sweden), and dissolved in ultra-pure water (ELGA LabWater, Marlow, UK). MAs were separated and quantified by high performance anion exchange chromatography–mass spectrometry (Dionex ICS 5000 – MSQ Plus™, Thermo Scientific, Waltham, US) with the internal standard method using mass labelled $^{13}C_6$-levoglucosan. We improved the chromatographic separation of the previously published method (Kirchgeorg et al., 2014) by using a CarboPac™ MA1 column (Thermo Scientific, 2 × 250 mm) and an AminoTrap column (Thermo Scientific, 2 × 50 mm). Chromeleon 6.8 Chromatography data system (Thermo Scientific) was applied for data acquisition and elaboration. All modifications of the original method are given in the Supporting information.

The total organic carbon was analysed by an aliquot of 100 mg of each freeze dried sample, following the EPA procedure (EPA

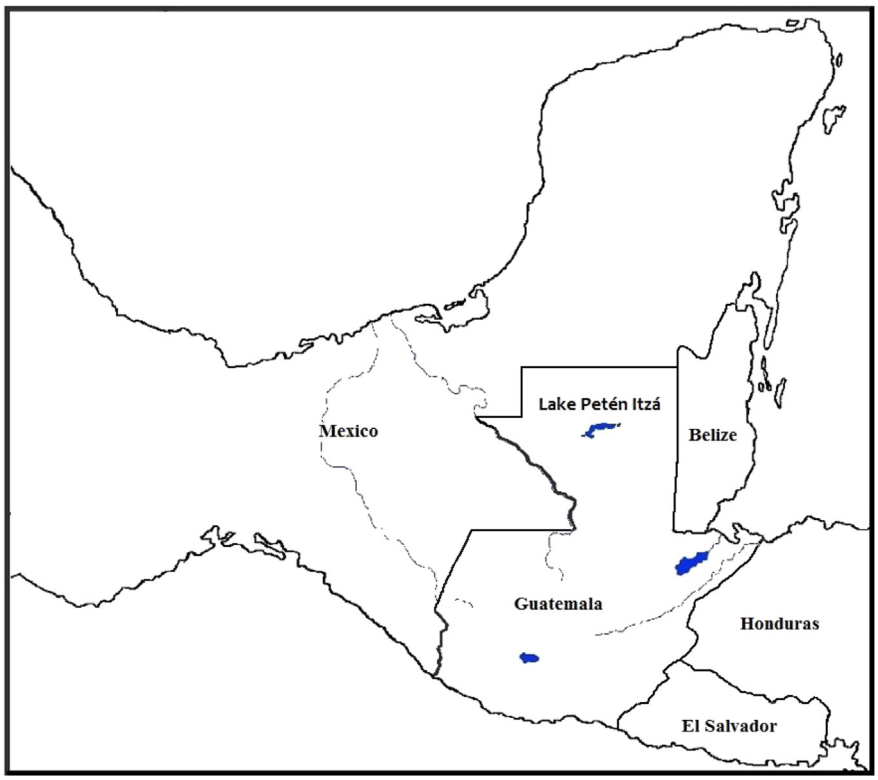

Fig. 1. Map of Mesoamerica, showing the study site at Lake Petén Itzá, Guatemala.

Method 9060). Inorganic carbon was removed prior to analysis by adding hydrochloric acid (2.5N) to the sample and then incubating it for 30 min at 120 °C. Excessive water was removed by oven-drying the sample at 105 °C overnight. Finally the dried sample was analysed with the TOC elemental analyser (TOC 5050, Shimadzu), by combustion at elevated temperatures using air as carrier gas. The CO_2 produced was measured by Fourier transform infrared spectroscopy.

Macroscopic charcoal analyses were performed at the University of Bern, Switzerland. For the analyses, 1 cm^3 of wet sample was first soaked for several hours in a deflocculating solution (5% sodium hexametaphosphate), treated with hydrogen peroxide (10%) for approx. 12 h to remove the organic content, and sieved over a 100 μm mesh. Macroscopic charcoal particles were estimated under a stereomicroscope at 40× magnification. We distinguished different types of charcoal morphotypes as in Colombaroli et al. (2014). Grass cuticles usually occur in flat sheets, and epidermal cells are arranged in parallel rows, with stomata within the rows (Jensen et al., 2007), and mostly have a length to width ratio ≥ 4:1 (Umbanhowar and Mcgrath, 1998). Woody material presents a thicker structure than the grass cuticle and the length to width ratio is normally lower (<4:1; Umbanhowar and Mcgrath, 1998). Leaf fragments can be separated from other charred material due to the presence of leaf veins, which are characterized by a divergence of the branches from a node (Jensen et al., 2007). Further details can be found in Beffa (2012) and Colombaroli et al. (2014).

3.3. Age-depth model

We calculated the depositional time (yrs cm^{-1}) of each level, using CLAM Version 2.2 (Blaauw, 2010), applying a spline interpolation (1000 iterations) between neighbouring levels and calibrating with the northern hemisphere terrestrial calibration curve from Reimer et al. (2013). Radiocarbon data (a total of 12 ^{14}C dates) from this and a parallel core were published by Mueller et al. (2009) and Hillesheim et al. (2005). Ten out of these 12 ^{14}C dates had been determined on a parallel core (11A), and only two on the 11B core. The core 11A covers about the same age and is about equally long as 11B, and it has been drilled 500 m north of 11B during the same drilling campaign in June 2002. However, from 11A the top 50 cm are missing (corresponding to about 600 years), whereas for 11B only the top 18 cm (approximately 200 years) are missing, see (Hillesheim et al., 2005; Anselmetti et al., 2006) for a detailed description of the various cores drilled along seismic line 11 in Lake Petén Itzá. The dates determined on the 11A core were projected onto the 11B core by matching visual stratigraphy by Mueller et al. (2009). One of the two dates determined on the 11B core was based on a charcoal sample (at 365 cm depth, 6735 cal yr BP), which we have discarded for our age model calculations because charcoal samples often show a bias towards older ages. All other samples were either wood pieces (ten) or leaves (one).

Different smoothing factors for the upper and the lower core sections have been chosen to better constrain rapid change in accumulation rates in the upper section, due to erosion (Maya Clay layer, e.g. Anselmetti et al., 2007; Mueller et al., 2009). We used 0.2 as a spline interpolation smoothing factor (Blaauw, 2010) for the upper section (up to and including the Maya Clay layer, i.e. approx. 3100 cal yr BP), and a 0.4 smoothing factor below the Maya Clay layer. In the lower core section we applied a slightly stronger smoothing in order to smooth out additional uncertainties introduced by the projection of the 11A ^{14}C dates onto the 11B core. Alternative age models including all ^{14}C dates and applying different smoothing factors illustrating the effect on the flux records are included in the Supplementary information.

The resulting depth-age model is shown in Fig. 2. We applied the depth-age model to calculate the fluxes of charcoal

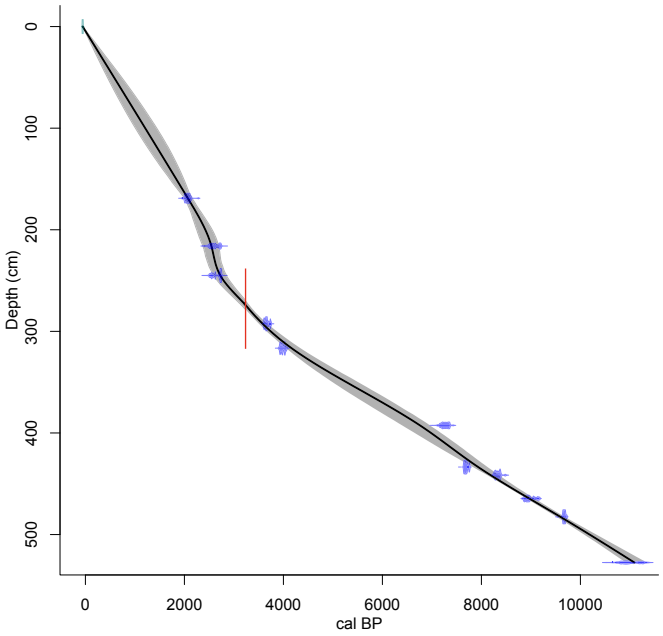

Fig. 2. Depth-age model based on eleven radiocarbon determinations and produced using CLAM 2.2 (Blaauw, 2010). The shift in the smoothing factor from 0.2 to 0.4 is indicated by the vertical red line. (For interpretation of the references to colour in this figure legend, the reader is referred to the web version of this article.)

(pieces cm^{-2} yr^{-1}) and of levoglucosan, mannosan and galactosan (ng cm^{-2} yr^{-1}).

4. Results

In this section we present the results of the charcoal and MA analyses performed on the PI 5 VI 02 11B core. Additionally, the total organic carbon (TOC) profile of the core is shown in Fig. 3. The TOC in the entire core is between 1 and 10 % which is in agreement with the values in the Petén Itzá sediment cores which were discussed by Mueller et al. (2009). It also shows the typical Maya clay layer (approx. 3000–1000 cal yr BP) with low TOC content observed in many Petén lake cores (e.g. Islebe et al., 1996; Curtis et al., 1998; Rosenmeier et al., 2002; Anselmetti et al., 2006). This inorganic clay layer is generally attributed to soil erosion resulting from ancient Maya forest clearance (Anselmetti et al., 2007; Mueller et al., 2009).

4.1. Charcoal

Macroscopic charcoal was detected in all investigated samples. Different morphotypes were distinguished when counting the charcoal particles (see "Materials and Methods"). Charcoal particles were mainly grasses (79% of total charcoal pieces), the second most important morphotype was wood-like charcoal (20%), and finally leaves, needles and others materials accounted for less than 1% of the total number of charcoal pieces. Total charcoal and the two main morphotypes of wood and grass concentrations are shown in Fig. 3, with concentrations between 0–176 pieces cm^{-3} and 1–582 pieces cm^{-3}, respectively.

In general, trends of charcoal fluxes (Fig. 4) mirror original concentrations, with the two main peaks at 370 cm (6100 cal yr BP) and 305 cm (3700 cal yr BP). However, the calculated charcoal fluxes are complemented by a third and less prominent peak at 225 cm (2600 cal yr BP), which is not visible in charcoal concentration records and is a result of the different deposition rates during this period. In the bottom section of the core the charcoal flux is very low (<2 pieces cm^{-3} yr^{-1}), demonstrating a slightly increasing trend with time. The trend of total charcoal flux of the bottom section is in good agreement with the charcoal data of the same core in the age interval 11k–5k cal yr BP presented by Hillesheim et al. (2005). Over the entire core the highest charcoal fluxes were found between 210 and 400 cm (2500–7000 cal yr BP). All charcoal types show a similar phasing during the first peak around 370 cm. Interestingly, during the second maximum around 305 cm the different charcoal types show a different pattern: They start to increase simultaneously at the onset of the increase of total charcoal around 305 cm, but the percentage of woody charcoal suddenly drops, while grass-like charcoal concentrations still increase before slowly decreasing after reaching its peak value (see Figs. 3 and 4). Above the second maximum, and especially above 250 cm, total charcoal influx is dominated by grass-like charcoal. In general, the two charcoal morphotypes follow a similar trend over the entire depth range. However, in the top 250 cm charcoal particles are almost exclusively grass-like particles (>90%), whereas from 300 cm downwards wood-like charcoal is relatively more abundant (approx. 75% grass vs. 25% wood).

4.2. Monosaccharide anhydrides

As in the charcoal record, the MA concentrations are generally low in the upper part of the core, as well as in the bottommost part (Fig. 3), and at an elevated level in the middle part from 300 to 490 cm (3700–9900 cal yr BP). In contrast to charcoal the MA concentrations show no clear maximum during this period, apart from galactosan around 400 cm (7000 cal yr BP). It is evident that levoglucosan and mannosan start to increase at 10k–9.5k cal yr BP and, thus, well before charcoal which begins to increase at 7000 cal yr BP and galactosan which begins to increase at 8000 cal yr BP. The highest values of levoglucosan concentrations are reached at 400 cm, after which it slowly decreases until dropping at 305 cm (3700 cal yr BP) along with TOC and (mainly wood-like) charcoal. In the upper half of the core, where low charcoal and MA concentrations prevail, slightly elevated levoglucosan concentrations can be observed between 200 and 80 cm depth (2400–960 cal yr BP). These elevated levoglucosan concentrations are even more evident in the flux record in Fig. 4. While the charcoal flux is constantly low after the 2600 cal yr BP peak, levoglucosan remains at an elevated level, although with a downward trend. Levoglucosan flux reaches its local minimum around 900 cal yr BP, after which it increases again along with mannosan and galactosan.

Generally, the three distinct maxima in the charcoal flux record are mirrored in the levoglucosan flux record, although the first levoglucosan maximum occurs approximately one thousand years before the charcoal maximum. Around 6000 cal yr BP, where sediment charcoal peaks for the first time, a local maximum in the levoglucosan flux is also evident. This levoglucosan peak height is in good agreement with the height of the charcoal peak relative to the two other peaks of charcoal and levoglucosan.

The flux records of the two isomers mannosan and galactosan significantly correlate with levoglucosan (R^2 = 0.53 and 0.46, respectively, p-values of $9.2 \cdot 10^{-10}$ and $2.8 \cdot 10^{-8}$, respectively, with N = 52 data points) during the middle section (7000–2000 cal yr BP), whereas in the bottom and the top sections the isomers trends differ from one another. While levoglucosan shows a constant increase from 10k–8k cal yr BP, galactosan shows only a slow increase at the beginning and then abruptly increases by a factor of 4 within about five centuries after ~8000 cal yr BP. Mannosan on the other hand increases faster in the oldest core section, but peaks at 8300 cal yr BP. Between 2000 and 800 cal yr BP the three isomers

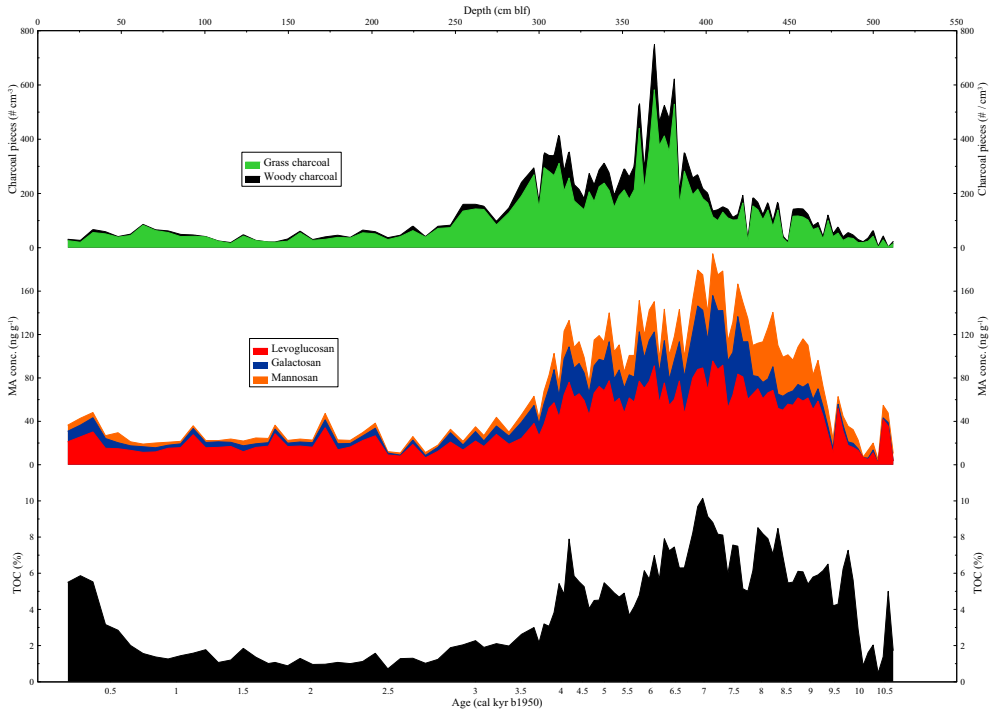

Fig. 3. Top: Concentrations of charcoal particles (black: woody charcoal, green: grass-like charcoal). Middle: Concentrations of MAs (red: levoglucosan, blue: galactosan, orange: mannosan), Bottom: Total Organic Content in the 11B core. All species are shown linearly versus depth (top axis), at the bottom the corresponding age is indicated. (For interpretation of the references to colour in this figure legend, the reader is referred to the web version of this article.)

appear to be completely uncorrelated, however, after 800 BP they all increase together, even though mannosan is not increasing as fast as the other two. The concentrations of the three isomers are influenced by the type of burned vegetation and the burning conditions (mainly temperature) (Fabbri et al., 2009 and references therein; Alves et al., 2010 and references therein; Kuo et al., 2011a). The abundance of the isomers is discussed in more detail in Sect. 5.

5. Discussion

The fire proxy records from Lake Petén Itzá represent fire history in lowland Guatemala during the entire Holocene. Here, we compare the fire history results with Holocene natural and human induced vegetation changes.

Before the transition into the Holocene, climate in Central American lowlands was probably drier and 4–8 °C cooler than during the early Holocene (e.g. Brenner et al., 2002; Hodell et al., 2008). At the transition into the Holocene the climate shifted to warmer and wetter conditions (Hodell et al., 2008), and the period from the early to the mid-Holocene (10–4.5 ka BP) was dominated by relatively stable warm and wet climate conditions (Hillesheim et al., 2005; Mueller et al., 2009). Pollen studies from Petén Department indicate that the vegetation shifted towards tropical forest from ~12.5 ka BP onwards, and that it was established by about 10 ka BP (e.g. Leyden et al., 1994; Hillesheim et al., 2005). Also based on pollen studies Islebe et al. (1996) found that a semi-evergreen and closed-forest (*Urticaceae* and *Moraceae*) was already established by ~8600 yr BP surrounding Lake Petén Itzá.

Fire activity was low during this transition of vegetation to tropical forest. The charcoal record demonstrates low values with a slightly increasing trend, whereas levoglucosan starts at low values at the very beginning of the Holocene but shows a substantially stronger increase during the early Holocene. The increasing fire activity may be explained by advancing forestation and subsequent higher fuel abundance.

Different behaviour at different burning conditions might be a reason for differences between MA and charcoal concentrations in the sediment. It is known that levoglucosan generation peaks at 250 °C and is not present in char above 350 °C, and galactosan and mannosan generation is peaking at 200 °C, depending on the burned vegetation type (Kuo et al., 2008, 2011a). On the other hand, charcoal is assumed to be generated at temperatures between 250 °C–500 °C. The earlier increase of the molecular markers might therefore be a result of low temperature and smouldering fires prevailing in the region during the early Holocene, which is captured less efficiently by the sediment charcoal proxy. This would be in line with more opened stands in the highlands of Guatemala because it was typically drier there during that period. In open stands, low intensity fires are prevailing and would thus explain an earlier increase of the MAs compared to sedimentary charcoal.

The different catchment areas of MAs compared to charcoal may also explain the observed differences among the two proxies. Macroscopic charcoal is usually transported only a few hundred meters to a few kilometres and is thus mostly a local fire proxy (Whitlock and Larsen, 2001), whereas levoglucosan can be transported as aerosol hundreds of kilometres and is therefore a regional to hemispheric fire proxy which integrates supra-regional fires (Zennaro et al., 2014). Therefore, the earlier increase of the MAs compared to charcoal might also be attributed to an increased fire activity linked to the forestation over the entire region of Mesoamerica or southern North America and not only in the lowlands near Lake Petén Itzá. Regional charcoal syntheses demonstrate that early-Holocene fire activity was not homogenously distributed over Central and North America and depended instead on regional climate conditions and occupation history (Power et al., 2012; Marlon et al., 2013). At Lake Ixtacola, Mexico, charcoal starts to increase at approx. 9500 cal yr BP (Piperno et al., 2007), whereas in

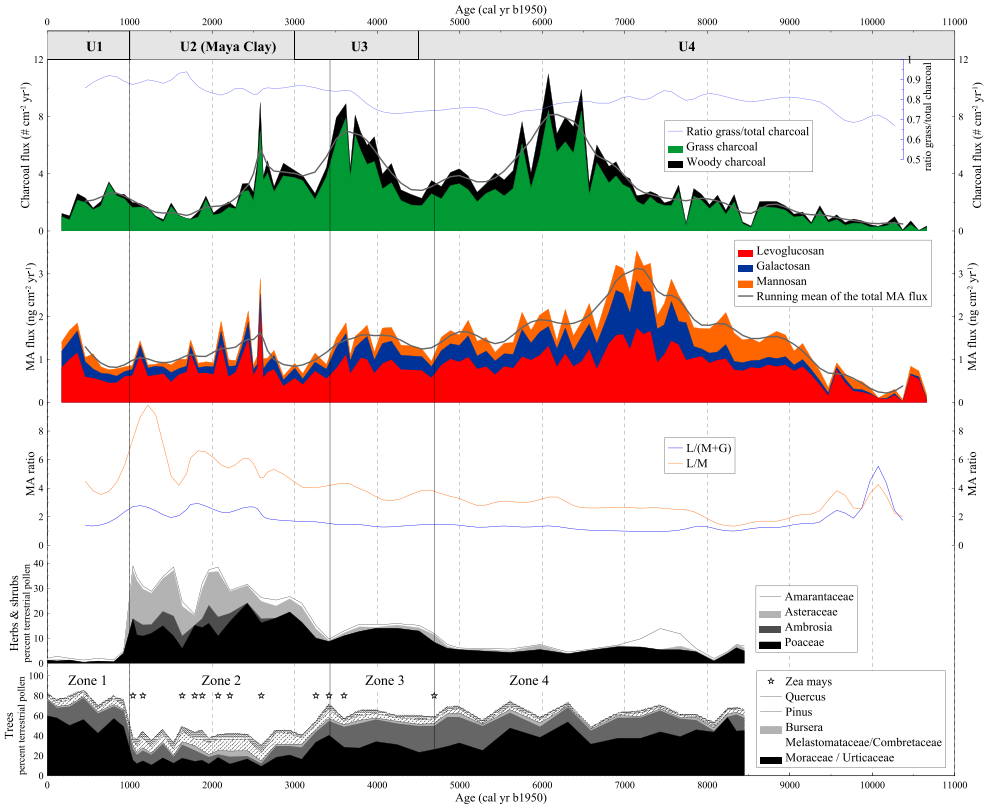

Fig. 4. Top: Grass charcoal (green) and woody charcoal (black), total charcoal corresponds to the upper envelope of the woody charcoal line. The ratio of grass to total charcoal is indicated as a blue line on a separate axis. The grey line indicates a 7-point Gaussian running mean of the total charcoal flux. Middle: Fluxes of MAs (red: levoglucosan, blue: galactosan, orange: mannosan). The grey line indicates a 7-point Gaussian running mean of the total MA flux. The ratio of levoglucosan/(mannosan + galactosan) (L/(M + G)) is shown as solid orange line, and the levoglucosan/mannosan (L/M) ratio is shown as solid blue line. Both ratios are indicated as 7-point Gaussian running means of the raw signal. Bottom: Pollen records from Lake Puerto Arturo (Wahl et al., 2006) are subdivided into grass and shrub pollen types (upper panel) and in arboreal pollen types (bottom panel). In the arboreal pollen panel, filled colours correspond to local trees, whereas hatched areas indicate disturbance arboreal types. Stars indicate core sections where *Zea mays* has been encountered. Pollen Zones as defined by Wahl et al. (2006) are indicated by black vertical lines, see text for details. On top the lithologic and lithostratigraphic units described in detail by Hillesheim et al. (2005) and Mueller et al. (2009) are indicated (U1: organic rich silt; U2: low organic content Maya Clay layer; U3: Deep water carbonate; U4: Organic-rich clay). All records are plotted linearly versus age. (For interpretation of the references to colour in this figure legend, the reader is referred to the web version of this article.)

a core from the Upper Lerma, Mexico, charcoal maxima were detected between 7000 and 8500 cal yr BP (Lozano-García et al., 2005), and finally, Lozano-García et al. (2013) found charcoal peaks around 9200 and 8000 cal yr BP in western central Mexico.

An additional reason for different behaviour of the MAs and charcoal may be different sedimentation and/or post-depositional processes, like the redistribution by pore-water, the potential biodegradation (Xie et al., 2006) or degradation processes depending on different sediment types (e.g. low organic content vs. organic rich sediment), which, however, have not been studied so far. Recent laboratory experiments observed degradation of dissolved levoglucosan in water (Norwood et al., 2013), but previous studies assumed that MAs attached to particles are stable enough for sedimentation and stored over long time scales in lake sediments (Elias et al., 2001). These post-depositional processes would influence the MA concentrations over the entire core; however, such trends in the MA concentrations were not observed in the core studied here.

The relative abundance of the different isomers and in particular the ratios between levoglucosan/mannosan and levoglucosan/(mannosan + galactosan) may be due to the type of vegetation burning and the burning conditions, mainly temperature of the fire (Fabbri et al., 2009 and references therein; Alves et al., 2010 and references therein; Kuo et al., 2011a). Oros et al. (2006) and Oros and Simoneit (2001a, b) reported MA ratios between 2–33 (average 14) for different types of grasses and 0.2–8.2 (average 4.9) for different types of hardwood; Engling et al. (2006) reported ratios of L/M = 108 and L/(M + G) = 54 for savannah grass, and L/M = 28 and L/(M + G) = 14 for hardwood (Oak), and Kuo et al. (2011a) reported ratios depending on the fire temperature. At the temperature of the levoglucosan production maximum (250 °C) cordgrass shows ratios of 36 for L/M and 13 for L/(M + G), respectively, and honey mesquite (hardwood) shows ratios of 4.4 for L/M and 1.3 for L/(M + G), respectively. Comparing all studies mentioned above, the reported ratios are overlapping, which limits conclusions about prevailing vegetation based on these ratios. Nevertheless, in all these studies grass shows higher MA ratios compared to hardwood. Considering this tendency, higher ratios in the present study may be an indication for an increased amount of grass being burned relative to wood, if not influenced by temperature. The MA ratios in our samples (Fig. 4) are highly variable in the early Holocene (10.5k–9k cal yr BP; L/M 0.4–11; L/(M + G) 0.5–15.5) and decrease until ~8200 cal yr BP, where they reach values of 1.2 (L/M) and 0.9 (L/(G + M)), respectively. The high variability might be due to the changing wet and dry cycles during this period as described by Hillesheim et al. (2005). However, in this section MA concentrations are close to or even at the detection limits of our analytical setup, therefore this part of the record should be interpreted carefully due to potential contamination and biases of the low concentration data. The ratios stabilise from 8000 cal yr BP onwards, when the vegetation has changed to more stable forest vegetation (Hillesheim et al., 2005).

The timing and sequence of Holocene fire history presented here correspond well with sediment charcoal from Lake Petén Itzá presented by Correa-Metrio et al. (2012) (entire Holocene), and Hillesheim et al. (2005) (10.5k–5k cal yr BP). The first maximum in the charcoal record and its corresponding levoglucosan peak around 6000 cal yr BP indicate the first local Holocene fire maximum detected in the Petén Itzá core. Correa-Metrio et al. (2012) proposed a period of high fire activity in Mesoamerica between 10.5k–5k cal yr BP and attribute the increasing fire activity to rising temperatures at the onset of the Holocene. In addition to higher temperatures Correa-Metrio et al. (2012) also link the fire activity to more pronounced seasonality related to the insolation maximum during this period which may have increased fuel availability and intensified convective storms facilitating ignition at the beginning of the wet season. Based on the absence of anthropogenic pollen indicators suggesting the presence of humans at Petén during that period (i.e. no *Zea mays*) (e.g. Leyden, 2002; Wahl et al., 2006), we attribute the change in the fire regime in the early to mid-Holocene, including the fire maximum around 6 ky BP, mainly to climate. The slow decrease of grass-like charcoal contribution to total charcoal abundance during this fire maximum is consistent with a gradual shift towards tropical high forest recorded in various pollen records (e.g. Islebe et al., 1996; Leyden, 2002; Mueller et al., 2009). Grass-like charcoal decrease does not seem to be affected by the extensive fire activity prevailing at that time. This decrease is also present in the pollen records (Islebe et al., 1996; Leyden, 2002; Wahl et al., 2006; Mueller et al., 2009).

During the relatively stable (in sense of temperature and moisture) mid-Holocene (~7–4.5 ka BP), the vegetation in Petén slowly shifted to more open, savannah-like type (e.g. Islebe et al., 1996; Leyden, 2002; Wahl et al., 2006), which may explain the slight increase of the MA ratios (L/M: from 2.7 to 3.2, L/(M + G): from 1.0 to 1.4) during this period. During the mid-Holocene, fire activity remains at a low level after the initial charcoal and levoglucosan peak, until abruptly increasing before 4000 cal yr BP. At the beginning of this increase in fire activity the abundance of grass-like charcoal is relatively low (70–80 % of total charcoal) (Fig. 4, top panel). In contrast to the first fire maximum (6500–5500 cal yr BP) where the contribution of grass-like charcoal to total charcoal counts decreases gradually, the grass-like charcoal percentage increases abruptly from below 75% to above 85% within less than 300 years simultaneously with this second distinct fire maximum around 3700 cal yr BP.

The rapid increase in grass-like charcoal at 3700 cal yr BP coincides with the fire maximum and a relatively fast shift from mostly tree towards herb and shrub pollen as observed by Islebe et al. (1996) and Mueller et al. (2009). This increase in herbaceous pollen types is also visible in the pollen record of Lake Puerto Arturo in northern Petén about 70 km away from Lake Petén Itzá (Wahl et al., 2006) shown in Fig. 4. The four zones in the pollen diagram defined by Wahl et al. (2006) correspond to periods of high arboreal pollen abundance (zone 4, older than 4700 cal yr BP), the start of a significant increase in herbaceous pollen types (zone 3, 4700–3400 cal yr BP), amplification of the shift towards more herbaceous and less arboreal pollen types and presence of anthropogenic indicators (*Z. mays* and *Ambrosia*) (zone 2, 3400–1000 cal yr BP), and an abrupt change from herbaceous and disturbance taxa back to arboreal pollen types (zone 1, after 1000 cal yr BP). The above mentioned abrupt shift in the charcoal types corresponds to the change in the pollen profile from arboreal towards more herbaceous pollen types in the transition from zone 3 into zone 2. Considering the age uncertainties of the two sediment cores (approx. 500 yr of two sigma age range at 3200 cal yr BP) in the Lake Puerto Arturo sediment (Wahl et al., 2006) and 100 yr at 3500 cal yr BP in the Petén Itzá 11B core, the abrupt shifts in the pollen records and in the fire proxy records are likely to happen simultaneously. Also the distinct decrease in *Brosimum* (Mueller et al., 2009) (not shown) fits temporally to the rapid change in the vegetation seen in the other records. This shift in the pollen records and the increase of grass-like charcoal coincide also with an increase of the MA ratios in this period (L/M up to 5.2, L/(M + G) up to 1.7) and might be a result of enhanced burning of grass-like vegetation. Local climate became drier in the period 4.5–3 ka BP (Mueller et al., 2009), which may have exacerbated the effect of human impact on vegetation. However, the shift towards direr climate and was a gradual process persistent during ~1.5 ka, whereas the changes in the pollen records and the distinct increase in grass-like charcoal took place within a few hundred years.

Initial evidence of agricultural activities in the Maya lowlands are dated to 4000–5000 BP, based on pollen studies where the increase of disturbance taxa (e.g. *Asteraceae* and *Ambrosia*) and of secondary forest taxa is attributed to forest clearance or is based on the presence of *Z. mays* which is an indicator for agricultural cultivation (e.g. Pope et al., 2001; Leyden, 2002; Wahl et al., 2006). Soil erosion histories point to a similar timing for the first appearance of human perturbation in the ecological system due to vegetation transformation (Anselmetti et al., 2007). The presence of a Maya Clay layer is a strong evidence for the presence of Maya settlements in the watershed of an investigated lake. In different lakes from the Petén region, such layers are present from about 3500 to 800 yr BP (Rosenmeier et al., 2002; Anselmetti et al., 2006; Mueller et al., 2009). The fact that the appearance of first human agricultural activities in the Maya lowlands is older than 4 ka BP indicates that the high fire activity at 3.7 ka BP may be attributed to humans rather than only climate. The presence of Maya clay layers in Petén lakes from ~3.5 ka BP onwards along with declining arboreal pollen abundance indicates that a considerable change in the vegetation occurred during that time. The coincident high fire activity provides a strong inference that fire clearance by early Maya populations may have started at this time. In general it is easier for humans to initiate fires in a drier environment, where the accompanying shift to a drier climate could have also favoured human-induced fires in this period. However, the first *Z. mays* pollen in Lake Petén Itzá or Lake Salpetén were found only after 3 ka BP (Leyden, 2002; Mueller et al., 2009). Thus, if the high fire activity in the area of Lake Petén Itzá around 3.7 ka BP is attributed to fire clearance by the Maya, this clearance would have happened considerably before the Maya started agricultural cultivation in this area. However, in Lake Puerto Arturo a single *Z. mays* grain was found at 4600 cal yr BP (Wahl et al., 2006), thus considerably earlier than in Lake Petén Itzá (Fig. 4, bottom panel). Wahl et al. (2006) discussed the early appearance of *Z. mays* at lake Puerto Arturo in the context of other early *Z. mays* appearances from coastal Veracruz around 7100 cal yr BP (Pope et al., 2001) and from nearby Belize as early as 5500 cal yr BP (Pohl et al., 1996). Another explanation for the different timing of the first appearance of *Z. mays* mentioned by Wahl et al. (2006) are the different sizes of the investigated lakes. Lake Puerto Arturo is small compared to Lake Petén Itzá, therefore the large size of the Petén lakes may have reduced the visibility of the weak *Z. mays* signal at 4600 cal yr BP. In summary, we conclude that the high fire activity in the Maya lowlands around 4000–3500 cal yr BP cannot be attributed clearly to either climate or human activities based on the data presented in this study and is likely to be influenced by both climate and humans.

The last of the three fire maxima at 2.7 ka BP observed in our proxy records lies well within the Maya Clay layer and corresponds with the maximum in the soil erosion rate (Anselmetti et al., 2007). Permanent Maya settlements and agriculture were established in the entire Maya lowlands at the mid-Preclassic period (about

2900–2400 yr BP). Even though the Maya population increased significantly only from the late-Preclassic onwards (2400–1750 yr BP), the local fire activity remains low after 2400 yr BP. This low fire activity can be explained by the low abundance of trees, seen e.g. in the low wood charcoal percentage as well as from the pollen assemblages from the Petén region (Fig. 4). Wahl et al. (2006) denoted the period from 3400 to 1000 cal yr BP as Zone 2 which is characterised by very low abundance of arboreal pollen and dominated by herbaceous and shrub pollen types and the presence of agricultural indicators (*Z. mays* and *Ambrosia*) (Fig. 4). In Zone 2 we also detected the lowest abundances of wood charcoal, i.e. total charcoal is dominated by grass like pieces (>90% in 2000–1000 cal yr BP), which is in line with the pollen records. Such grassland vegetation negates the need for extensive fire clearance. However, the regional fire signal (levoglucosan, see Fig. 4) remains at an elevated level with a steadily decreasing trend, which might be caused by a further expansion of the Maya settlements at the borders of the Maya territories. These additional fires would only be revealed in the levoglucosan and not in the charcoal record due to the different catchment areas of the two fire proxies. In addition, MA ratios demonstrate an elevated level (L/M is between 3 and 10, L/(M + G) is between 1.5 and 3.5) and high variability during this period. This variability may be an indication of a disturbance of the natural fire activity by the Maya by influencing e.g. type of burned biomass or fire conditions and intensity, which results in different MA ratios (Engling et al., 2006; Kuo et al., 2011a), because the period before the assumed arrival of the Maya at Lake Petén Itzá was characterized by quite stable (levoglucosan/(mannosan + galactosan)) or only slowly increasing (levoglucosan/mannosan) MA ratios, respectively. Based on the evidence as described in this paragraph, we attribute the elevated fire activity at 2.7 cal ka BP to fire clearance by the Maya.

After the *Classic Maya collapse* (~900 yr BP) the fire activity remains at a low level, probably accompanied by a natural forestation and, thus, build-up of fuel. As a consequence the wood charcoal percentage increases after 800 yr BP (Fig 4). After ~600 yr BP the fire activity starts to increase again, this is evident especially in the levoglucosan record. Also the MA ratios recover after the *Maya collapse* and they decrease towards values as before 4000 cal yr BP, clearly reproducing the rapid transition from mainly herbaceous to primarily arboreal pollen abundance as observed in the pollen records.

6. Conclusions

We provide a detailed reconstruction of biomass burning trends from the southern Maya Lowlands from a Lake Petén Itzá sediment core using two different fire proxies: macroscopic charcoal and the monosaccharide anhydrates levoglucosan, mannosan and galactosan. The combination of different fire proxies offers new insights into the fire history during the Holocene at different spatial scales across the Maya lowlands.

The Holocene fire record demonstrates a first period of high fire activity between 9000 and 6000 cal yr BP, which is attributed to climate conditions and corroborates corresponding results from previous studies. The fire maximum at 2700 cal yr BP can be linked to the agricultural activity of the Maya at Lake Petén Itzá. The fire maximum around 3700 cal yr BP might already be influenced by early anthropogenic agricultural activities in the region, based on the fast decrease in the relative abundance of wooden charcoal during the fire maximum. However, we cannot exclude that this fire maximum and the accompanying shift in the vegetation type were a result of the dry climate conditions facilitating ignition. To further constrain the causes for the high fire activity around 3700 cal yr BP further investigations including several lake cores from this area with highly resolved data are needed.

An advantage of analysing MAs together with charcoal in lake sediments is the potential discrimination of different catchment areas of the proxies: While macroscopic charcoal represents a local fire signal, the MA record is influenced by regional to supra-regional fires, thus overlapping the spatial scale covered by microscopic charcoal (Whitlock and Larsen, 2001; Colombaroli et al., 2008; Conedera et al., 2009). Furthermore, higher concentrations in MAs might indicate that low temperature fires (<350 °C) where prevailing, while charcoal production is more efficient at temperatures between 250° and 500 °C. Analysing all three isomers enables the calculation of L/M and L/(M + G) ratios, which may help to estimate changes in types of burned vegetation. However, such conclusions are limited to the identification of general vegetation changes (wood vs. grass) and cannot identify specific vegetation compositions due to their temperature dependence and due to the large ranges of these ratios reported in the literature. Nevertheless, the promising correlation between the Petén Itzá MA ratios, pollen assemblages, and plant macrofossils demonstrates the added value of these molecular markers in paleo fire reconstructions.

Acknowledgements

The research leading to these results has received funding from the Swiss National Science Foundation (project No. 142063) and the European Research Council under the European Union's Seventh Framework Programme (FP7/2007-2013)/ERC Grant agreement No. 267696 – "EARLYhumanIMPACT". This is EARLYhumanIMPACT contribution 14.

The authors would like to thank Jason Curtis for subsampling the sediment core, and Roberta Zangrando and Elena Barbaro for their valuable help in the laboratory. Furthermore, we would like to thank Thermo Scientific for providing the CarboPac™ MA1 column and their MSQ support and ELGA Lab water, High Wycombe, UK, for supplying the pure water systems used in this study.

Appendix A. Supplementary data

Supplementary data related to this article can be found at http://dx.doi.org/10.1016/j.quascirev.2015.03.004.

References

Alves, C.A., Gonçalves, C., Evtyugina, M., Pio, C.A., Mirante, F., Puxbaum, H., 2010. Particulate organic compounds emitted from experimental wildland fires in a Mediterranean ecosystem. Atmos. Environ. 44, 2750–2759.

Anselmetti, F.S., Ariztegui, D., Hodell, D.A., Hillesheim, M.B., Brenner, M., Gilli, A., McKenzie, J.A., Mueller, A.D., 2006. Late Quaternary climate-induced lake level variations in Lake Petén Itzá, Guatemala, inferred from seismic stratigraphic analysis. Palaeogeogr. Palaeoclimatol. Palaeoecol. 230, 52–69.

Anselmetti, F.S., Hodell, D.A., Ariztegui, D., Brenner, M., Rosenmeier, M.F., 2007. Quantification of soil erosion rates related to ancient Maya deforestation. Geology 35, 915–918.

Beffa, G., 2012. Analysis of Sediment Charcoal Morphotypes from Gorgo Basso (Sicily). Institute of Plant Sciences. University of Bern, pp. 1–13 (Bachelor thesis).

Blaauw, M., 2010. Methods and code for 'classical' age-modelling of radiocarbon sequences. Quat. Geochronol. 5, 512–518.

Bowman, D.M.J.S., Balch, J.K., Artaxo, P., Bond, W.J., Carlson, J.M., Cochrane, M.A., D'Antonio, C.M., DeFries, R.S., Doyle, J.C., Harrison, S.P., Johnston, F.H., Keeley, J.E., Krawchuk, M.A., Kull, C.A., Marston, J.B., Moritz, M.A., Prentice, I.C., Roos, C.I., Scott, A.C., Swetnam, T.W., van der Werf, G.R., Pyne, S.J., 2009. Fire in the earth system. Science 324, 481–484.

Brenner, M., Rosenmeier, M.F., Hodell, D.A., Curtis, J.H., 2002. Paleolimnology of the Maya Lowlands – long-term perspectives on interactions among climate, environment, and humans. Anc. Mesoam. 13, 141–157.

Carcaillet, C., Almquist, H., Asnong, H., Bradshaw, R.H.W., Carrión, J.S., Gaillard, M.J., Gajewski, K., Haas, J.N., Haberle, S.G., Hadorn, P., Müller, S.D., Richard, P.J.H., Richoz, I., Rösch, M., Sánchez Goñi, M.F., von Stedingk, H., Stevenson, A.C., Talon, B., Tardy, C., Tinner, W., Tryterud, E., Wick, L., Willis, K.J., 2002. Holocene

biomass burning and global dynamics of the carbon cycle. Chemosphere 49, 845–863.
Colombaroli, D., Ssemmanda, I., Gelorini, V., Verschuren, D., 2014. Contrasting long-term records of biomass burning in wet and dry savannas of equatorial East Africa. Glob. Change Biol. 20, 2903–2914.
Colombaroli, D., Vannière, B., Emmanuel, C., Magny, M., Tinner, W., 2008. Fire-vegetation interactions during the Mesolithic-Neolithic transition at Lago dell'Accesa, Tuscany, Italy. Holocene 18, 679–692.
Conedera, M., Tinner, W., Neff, C., Meurer, M., Dickens, A.F., Krebs, P., 2009. Reconstructing past fire regimes: methods, applications, and relevance to fire management and conservation. Quat. Sci. Rev. 28, 555–576.
Correa-Metrio, A., Bush, M.B., Cabrera, K.R., Sully, S., Brenner, M., Hodell, D.A., Escobar, J., Guilderson, T., 2012. Rapid climate change and no-analog vegetation in lowland Central America during the last 86,000 years. Quat. Sci. Rev. 38, 63–75.
Curtis, J.H., Brenner, M., Hodell, D.A., Balser, R.A., Islebe, G.A., Hooghiemstra, H., 1998. A multi-proxy study of Holocene environmental change in the Maya Lowlands of Peten, Guatemala. J. Paleolimnol. 19, 139–159.
Deevey, E.S., Brenner, M., Flannery, M.S., Yezdani, G.H., 1980. Lakes Yaxha and Sacnab, Petén, Guatemala: limnology and hydrology. Arch. Hydrobiol. 57, 419–460.
Elias, V.O., Simoneit, B.R.T., Cordeiro, R.C., Turcq, B., 2001. Evaluating levoglucosan as an indicator of biomass burning in Carajás, amazônia: a comparison to the charcoal record. Geochim. Cosmochim. Acta 65, 267–272.
Engling, G., Carrico, C.M., Kreidenweis, S.M., Collett Jr., J.L., Day, D.E., Malm, W.C., Lincoln, E., Min Hao, W., Iinuma, Y., Herrmann, H., 2006. Determination of levoglucosan in biomass combustion aerosol by high-performance anion-exchange chromatography with pulsed amperometric detection. Atmos. Environ. 40 (Suppl. 2), 299–311.
Fabbri, D., Torri, C., Simoneit, B.R.T., Marynowski, L., Rushdi, A.I., Fabiańska, M.J., 2009. Levoglucosan and other cellulose and lignin markers in emissions from burning of Miocene lignites. Atmos. Environ. 43, 2286–2295.
Haug, G.H., Günther, D., Peterson, L.C., Sigman, D.M., Hughen, K.A., Aeschlimann, B., 2003. Climate and the collapse of Maya civilization. Science 299, 1731–1735.
Hillesheim, M.B., Hodell, D.A., Leyden, B.W., Brenner, M., Curtis, J.H., Anselmetti, F.S., Ariztegui, D., Buck, D.G., Guilderson, T.P., Rosenmeier, M.F., Schnurrenberger, D.W., 2005. Climate change in lowland Central America during the late deglacial and early Holocene. J. Quat. Sci. 20, 363–376.
Hodell, D.A., Anselmetti, F.S., Ariztegui, D., Brenner, M., Curtis, J.H., Gilli, A., Grzesik, D.A., Guilderson, T.J., Müller, A.D., Bush, M.B., Correa-Metrio, A., Escobar, J., Kutterolf, S., 2008. An 85-ka record of climate change in lowland Central America. Quat. Sci. Rev. 27, 1152–1165.
Islebe, G.A., Hooghiemstra, H., Brenner, M., Curtis, J.H., Hodell, D.A., 1996. A Holocene vegetation history from lowland Guatemala. Holocene 6, 265–271.
Jensen, K., Lynch, E.A., Calcote, R., Hotchkiss, S.C., 2007. Interpretation of charcoal morphotypes in sediments from Ferry Lake, Wisconsin, USA: do different plant fuel sources produce distinctive charcoal morphotypes? Holocene 17, 907–915.
Kennett, D.J., Breitenbach, S.F.M., Aquino, V.V., Asmerom, Y., Awe, J., Baldini, J.U.L., Bartlein, P., Culleton, B.J., Ebert, C., Jazwa, C., Macri, M.J., Marwan, N., Polyak, V., Prufer, K.M., Ridley, H.E., Sodemann, H., Winterhalder, B., Haug, G.H., 2012. Development and disintegration of Maya political systems in response to climate change. Science 338, 788–791.
Kirchgeorg, T., Schüpbach, S., Kehrwald, N., McWethy, D.B., Barbante, C., 2014. Method for the determination of specific molecular markers of biomass burning in lake sediments. Org. Geochem. 71, 1–6.
Kuo, L.-J., Herbert, B.E., Louchouarn, P., 2008. Can levoglucosan be used to characterize and quantify char/charcoal black carbon in environmental media? Org. Geochem. 39, 1466–1478.
Kuo, L.-J., Louchouarn, P., Herbert, B.E., 2011a. Influence of combustion conditions on yields of solvent-extractable anhydrosugars and lignin phenols in chars: Implications for characterizations of biomass combustion residues. Chemosphere 85, 797–805.
Kuo, L.-J., Louchouarn, P., Herbert, B.E., Brandenberger, J.M., Wade, T.L., Crecelius, E., 2011b. Combustion-derived substances in deep basins of Puget Sound: historical inputs from fossil fuel and biomass combustion. Environ. Pollut. 159, 983–990.
Leyden, B.W., 2002. Pollen evidence for climatic variability and culturaldisturbance in the Maya Lowlands. Anc. Mesoam. 13, 85–101.
Leyden, B.W., Brenner, M., Hodell, D.A., Curtis, J.H., 1994. Orbital and internal forcing of climate on the Yucatan Peninsula for the past ca. 36 ka. Palaeogeogr. Palaeoclimatol. Palaeoecol. 109, 193–210.
Lozano-García, S., Sosa-Nájera, S., Sugiura, Y., Caballero, M., 2005. 23,000 yr of vegetation history of the Upper Lerma, a tropical high-altitude basin in Central Mexico. Quat. Res. 64, 70–82.
Lozano-García, S., Torres-Rodríguez, E., Ortega, B., Vázquez, G., Caballero, M., 2013. Ecosystem responses to climate and disturbances in western central Mexico during the late Pleistocene and Holocene. Palaeogeogr. Palaeoclimatol. Palaeoecol. 370, 184–195.
Marlon, J.R., Bartlein, P.J., Daniau, A.-L., Harrison, S.P., Maezumi, S.Y., Power, M.J., Tinner, W., Vanniére, B., 2013. Global biomass burning: a synthesis and review of Holocene paleofire records and their controls. Quat. Sci. Rev. 65, 5–25.
Mueller, A.D., Islebe, G.A., Hillesheim, M.B., Grzesik, D.A., Anselmetti, F.S., Ariztegui, D., Brenner, M., Curtis, J.H., Hodell, D.A., Venz, K.A., 2009. Climate drying and associated forest decline in the lowlands of northern Guatemala during the late Holocene. Quat. Res. 71, 133–141.
Norwood, M.J., Louchouarn, P., Kuo, L.-J., Harvey, O.R., 2013. Characterization and biodegradation of water-soluble biomarkers and organic carbon extracted from low temperature chars. Org. Geochem. 56, 111–119.
Oros, D.R., Abas, M.R.b., Omar, N.Y.M.J., Rahman, N.A., Simoneit, B.R.T., 2006. Identification and emission factors of molecular tracers in organic aerosols from biomass burning: part 3. Grasses. Appl. Geochem. 21, 919–940.
Oros, D.R., Simoneit, B.R.T., 2001a. Identification and emission factors of molecular tracers in organic aerosols from biomass burning Part 1. Temperate climate conifers. Appl. Geochem. 16, 1513–1544.
Oros, D.R., Simoneit, B.R.T., 2001b. Identification and emission factors of molecular tracers in organic aerosols from biomass burning Part 2. Deciduous trees. Appl. Geochem. 16, 1545–1565.
Piperno, D.R., Moreno, J.E., Iriarte, J., Holst, I., Lachniet, M., Jones, J.G., Ranere, A.J., Castanzo, R., 2007. Late Pleistocene and Holocene environmental history of the Iguala Valley, Central Balsas watershed of Mexico. Proc. Natl. Acad. Sci. 104, 11874–11881.
Pohl, M.D., Pope, K.O., Jones, J.G., Jacob, J.S., Piperno, D.R., deFrance, S.D., Lentz, D.L., Gifford, J.A., Danforth, M.E., Josserand, J.K., 1996. Early agriculture in the Maya lowlands. Lat. Am. Antiq. 7, 355–372.
Pohl, M.E.D., Piperno, D.R., Pope, K.O., Jones, J.G., 2007. Microfossil evidence for pre-Columbian maize dispersals in the neotropics from San Andrés, Tabasco, Mexico. Proc. Natl. Acad. Sci. U. S. A. 104, 6870–6875.
Pope, K.O., Pohl, M.E.D., Jones, J.G., Lentz, D.L., Nagy, C.v., Vega, F.J., Quitmyer, I.R., 2001. Origin and environmental setting of ancient agriculture in the lowlands of Mesoamerica. Science 292, 1370–1373.
Power, M., Mayle, F., Bartlein, P., Marlon, J., Anderson, R., Behling, H., Brown, K., Carcaillet, C., Colombaroli, D., Gavin, D., Hallett, D., Horn, S., Kennedy, L., Lane, C., Long, C., Moreno, P., Paitre, C., Robinson, G., Taylor, Z., Walsh, M., 2012. Climatic control of the biomass-burning decline in the Americas after ad 1500. Holocene 23, 3–13.
Reimer, P.J., Bard, E., Bayliss, A., Beck, J.W., Blackwell, P.G., Bronk Ramsey, C., Buck, C.E., Edwards, R.L., Friedrich, M., Grootes, P.M., Guilderson, T.P., Haflidason, H., Hajdas, I., Hatté, C., Heaton, T.J., Hoffmann, D.L., Hogg, A.G., Hughen, K.A., Kaiser, K.F., Kromer, B., Manning, S.W., Niu, M., Reimer, R.W., Richards, D.A., Scott, E.M., Southon, J.R., Turney, C.S.M., van der Plicht, J., 2013. IntCal13 and Marine13 radiocarbon age calibration curves, 0–50,000 years cal BP. Radiocarbon 55, 1869–1887.
Rice, D.S., Rice, P.M., Pugh, T., 1998. Settlement Continuity and Change in the Central Peten Lakes Region: The Case of Zacpeten. In: Ruiz, A.C., et al. (Eds.), Anatomia de una Civilizacion: Aproximaciones Interdisciplinarias a la Cultura Maya. Sociedad Española de Estudios Mayas, Madrid, Spain, ISBN 978-84-923545-0-4, pp. 207–252.
Rosenmeier, M.F., Hodell, D.A., Brenner, M., Curtis, J.H., Guilderson, T.P., 2002. A 4000-year lacustrine record of environmental change in the southern Maya lowlands, Petén, Guatemala. Quat. Res. 57, 183–190.
Ruddiman, W.F., 2003. The anthropogenic greenhouse era began thousands of years ago. Clim. Change 61, 261–293.
Umbanhowar, C.E., Mcgrath, M.J., 1998. Experimental production and analysis of microscopic charcoal from wood, leaves and grasses. Holocene 8, 341–346.
Wahl, D., Byrne, R., Schreiner, T., Hansen, R., 2006. Holocene vegetation change in the northern Peten and its implications for Maya prehistory. Quat. Res. 65, 380–389.
Whitlock, C., Larsen, C., 2001. Charcoal as a fire proxy. In: Smol, J.P., Birks, H.J.B., Last, W.M. (Eds.), Tracking Environmental Change Using Lake Sediments. Kluwer Academic Publishers, Dordrecht, The Netherlands, pp. 1–23.
Xie, H., Zhuang, X., Bai, Z., Qi, H., Zhang, H., 2006. Isolation of levoglucosan-assimilating microorganisms from soil and an investigation of their levoglucosan kinases. World J. Microbiol. Biotechnol. 22, 887–892.
Zennaro, P., Kehrwald, N., McConnell, J.R., Schüpbach, S., Maselli, O.J., Marlon, J., Vallelonga, P., Leuenberger, D., Zangrando, R., Spolaor, A., Borrotti, M., Barbaro, E., Gambaro, A., Barbante, C., 2014. Fire in ice: two millennia of boreal forest fire history from the Greenland NEEM ice core. Clim. Past 10, 1905–1924.